A non-invasive diagnostic tool for cellulose acetate films using a portable miniaturized near infrared spectrometer

Title: *A non-invasive diagnostic tool for cellulose acetate films using a portable miniaturized near infrared spectrometer*

Authors: Marco Valente Chavez Lozano [a], Emilio Catelli[a], Giorgia Sciutto[a], Silvia Prati[a*], Emiliano Genorini[b] Rocco Mazzeo[a]

[a] *University of Bologna, Department of Chemistry "G. Ciamician", Ravenna Campus, Via Guaccimanni, 42–48121, Ravenna, Italy*

[b] *Viavi Solutions, Via Enrico Cernuschi 8, Monza, 20900, Italy*

**Corresponding author*
Email: s.prati@unibo.it
Work phone: +39 0544937153, Fax: +39 0544937159

Abstract:

This article tests the suitability of a new method to monitor the degree of substitution of cellulose acetate films, by employing a compact and inexpensive near-infrared miniaturized spectrometer (908.1–1676.2 nm) that can be easily applied in situ. The present study compares the analytical performance of the proposed method against conventional diagnostic strategies based on benchtop micro-attenuated total reflectance Fourier transform Infrared (μATR -FTIR) measurements in the mid-infrared spectral range.

The novel calibration function exploits the shifts in the first overtone of the hydroxyl stretching 2νOH band of probe materials and was created using a set of analytical standards with different degrees of substitution. The robustness of the method was assessed by application on a group of sixteen historical cinematographic films. The accurate condition assessment of these films was performed in situ, in a non-invasive manner. The proposed analytical procedure is quick and easy-to-implement, and therefore it constitutes a rapid method to guide conservation strategies regarding film storage and digitalization in cultural institutions, including museums and cinematheques. Potential applications on three-dimensional objects and industrial processes are possible.

Keywords: Non-destructive analysis; NIR portable spectrometer; Cellulose acetate degree of substitution; On site monitoring

Abbreviations: CA, Cellulose Acetate; CDA, Cellulose Diacetate; CTA, Cellulose Triacetate; MCC, Microcrystalline Cellulose; DS, Degree of Substitution; TPP, Triphenyl Phosphate; PET, Polyethylene Terephthalate; micro-Attenuated Total Reflectance Fourier Transform Infrared, μATR-FTIR

1. *Introduction*

Cellulose Acetate (CA) is a cellulose derivative where hydroxyl groups in the glucopyranose ring have been substituted by acetate groups CH_3COO^-. The average number of OH groups substituted by acetate groups is known as the degree of substitution (DS) and in commercial products ranges between 2.3 and 2.5, or between 2.9 and 3.0 [1].

CA has been employed mixed with flame retardants and plasticizers (i.e. phosphates and phthalates) to produce sunglasses, combs, brooches and jewelry cases, often imitating expensive materials like mother-of-pearl, ivory or tortoiseshell [2]. Since the twentieth century, CA was also used for producing transparent and flexible bases for photographic supports, called "safety films" due to their lower

flammability when compared to cellulose nitrate supports [3]. Therefore, CA is a very abundant material in cinematheques and photographic archives.

Unfortunately, CA is also intrinsically unstable and hence, its use has been progressively reduced and substituted with more stable plastics, such as polyethylene terephthalate (PET) [4]. CA objects pose serious threats to museum collections, as this polymer exhibits hydrolytic deterioration mechanisms which trigger the heterolytic scission of acetate substitutive groups from the CA chain [1] (Fig. 1). The resulting acetic acid further catalyzes the scission of acetate groups and the hydrolytic scission of the cellulose chains. Moreover, the developed acetic acid may affect also nearby materials.

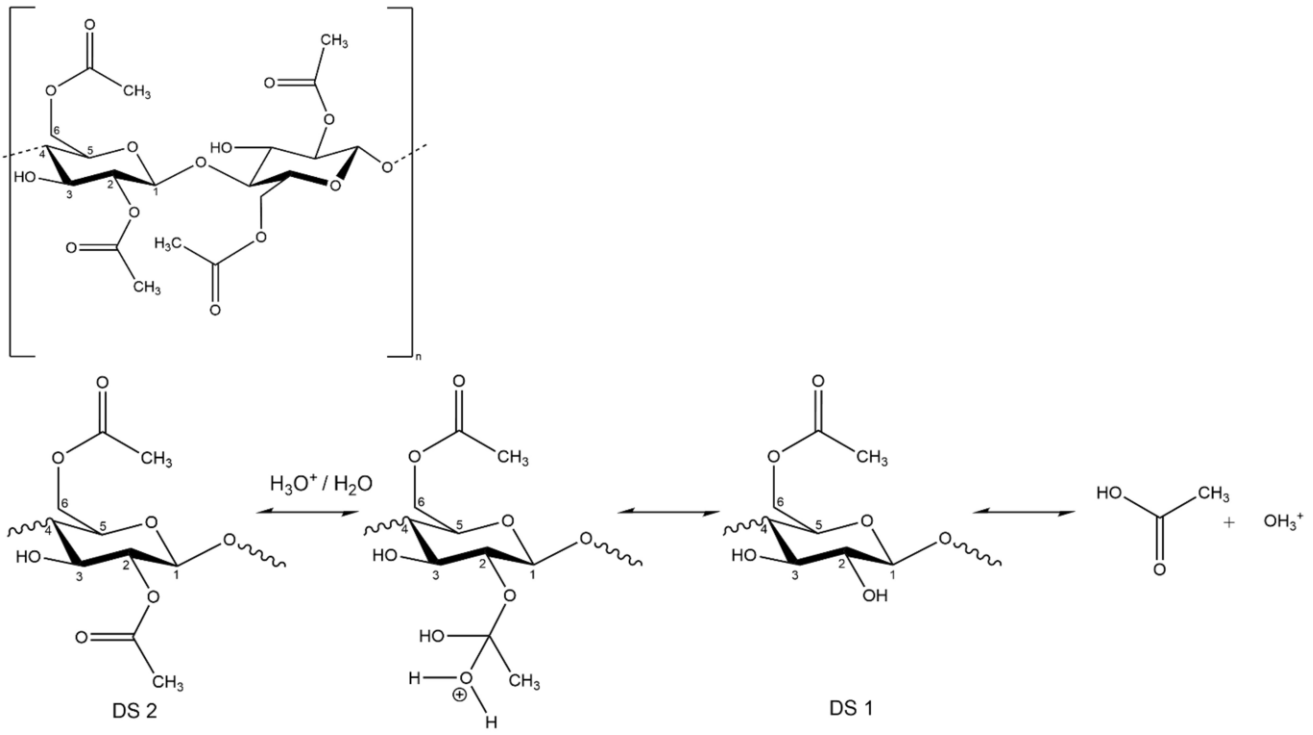

Fig. 1. Scheme illustrating the repeating structure of CA (up) and the polymer's hydrolytic breakdown mechanism (below).

These mechanisms develop quickly under uncontrolled storage conditions, particularly in unventilated environments with high temperature and relative humidity. As a consequence, CA objects may shrink and become distorted, frail and brittle; until the object finally crumbles down to dust [5]. To prevent the loss of CA artifacts and film bases, their accurate condition assessment and monitoring are key for heritage institutions, as these allow the design of suitable conservation strategies regarding display and storage conditions (i.e. cool or cold storages) [6].

Since hydrolysis is its primary degradation mechanism, monitoring the decrease of the DS of a CA based object may be used to gain information on the artifact's state of conservation[1].

On the other hand, the evaluation of the DS within a real historical object may be challenging and time consuming. The DS may be accurately measured by titration after alkaline hydrolysis of ester bonds to ascertain the percentage of combined acetic acid [7]. Nuclear magnetic resonance (NMR) and chromatographic techniques such as gas chromatographic analysis (GC) and ion chromatography (IC) have been reported to accurately quantify the DS in CA by measuring acetic acid content after removing any plasticizers by solvent extraction [8,9]. However, all these techniques require (sometimes considerable) sampling, becoming often unsuitable for the analysis of heritage objects. Moreover, the

sample pretreatment and experimental set-ups may be long, complex, and not easily employable for all museums or conservation institutes.

In previous researches [1,10], Fourier transform infrared (FTIR) spectroscopy both in transmission and macro-attenuated total reflectance (ATR) acquisition modes was used to calculate the DS of CA.

Microcrystalline cellulose (MCC), cellulose diacetate (CDA) standards, and their mixtures were analyzed to create a calibration curve by plotting the DS as a function of the ratio between a reference band, (*ν*COC), and OH stretching (*ν*OH).

It must be noted that, although ATR-FTIR offers the advantage of providing diagnostic information without the need of sampling, this type of analysis is restricted to the study of flat surfaces, in order to ensure good contact between the ATR crystal and the object. Furthermore, ATR-FTIR is a superficial technique which sample up to few microns from the surface [11] and thus it may lead to less representative results if the degradation is not homogenous at different depths.

To overcome the drawbacks of the already proposed methods, in this paper we propose the use of Near-infrared (NIR) spectroscopy to evaluate the state of conservation of cellulose acetate calculating its DS.

NIR spectroscopy allows to register overtone and combination bands related to a few functional group molecular vibrations in the NIR region (12500 to 4000 cm^{-1} or 800 to 2500 nm) [12], thus enabling the chemical characterization of both organic and inorganic materials. NIR spectroscopy is an extremely fast and cost-effective way to conduct molecular investigation of polymers, particularly when applied in the diffuse reflectance acquisition mode, and it is now widely employed for plastic waste classification at recycling facilities [13]. Recently several applications have been reported in the medical field [14-17] exploiting the higher penetration depth inside the sample when employing the 1000-1700 nm range (NIR-II), thanks to the reduction of light scattering and lower absorption occurring at this range, resulting in an increased signal-to-noise ratio. For cellulosic substrates, for instance, the point where the substrate response signal is reduced by 50% may range from 39 to 180 μm, with higher penetration corresponding to larger wavelengths [18] , thus enabling to acquire bulk information, whereas mid-infrared spectroscopy allows to obtain only superficial information [19,20].

However, despite its low cost and ease of application, this technique has not yet been widely implemented in the context of heritage institutions, due to the inherent complexity of the broad and poorly resolved overtone and combination bands, which often overlap.

In a previous paper by Catelli et al., NIR results proved useful for classifying heterogeneous artwork samples, showing highly specific responses for polymers in cinematographic film bases, which allowed for their identification [21] . The same research proved that, specifically for film bases constituted of CA, NIR spectroscopy was able to distinguish degraded CA films from better-preserved ones, showing promising capabilities as a tool for monitoring the state of conservation, with the advantages of being a non-invasive technique and requiring inexpensive and relatively simpler instrumentation than FTIR spectroscopy.

Aiming to obtain a fast and inexpensive way to monitor the condition of CA cinematographic and photographic films in heritage collections, we hereby propose a cheap, easy, fast and non-invasive method for diagnosing the DS of CA film bases, by employing a NIR calibration function built with a commercially available, portable and miniaturized NIR spectrometer which exploits the correlation between the DS and the position of the first overtone band of the OH stretching mode (2*ν*OH).

The employed NIR spectrometer operates in diffuse reflectance in the range 908.1–1676.2 nm. It is a small and light equipment (45 mm in diameter, 47.5 mm in height, and 60 g of weight), and therefore it can be easily employed in situ.

The effectiveness of the protocol was validated on real samples by comparing the results with those achieved with a µATR-FTIR calibration function obtained following the methodology proposed by Nunes et al. [1].

This protocol will be useful for the monitoring CA degradation processes, in order to support decision-making for preventive conservation strategies such as low-temperature storage in order to slow down the hydrolytic de-acetylation.

2. Materials and methods

2.1. Reference standards

The following materials were purchased to prepare the standards:

Cellulose triacetate (CTA, Fluka, DS 2.97), triphenyl phosphate (TPP, Sigma-Aldrich, ≥ 99%); cellulose diacetate (CDA, Sigma-Aldrich, DS 2.31, equivalent to an acetyl wight percent of 39.70%; water ≤ 3.0 %), microcrystalline cellulose (MCC, Sigma-Aldrich, C=11%).

In order to produce a µATR-FTIR calibration curve following the procedures reported in Nunes et al. [1], and for preparing the new NIR calibration function, three separate sets of 6 standard pellets were prepared using CDA (DS 2.31) and MCC (DS 0) powders mixed in the proportion reported in Table 1.

N°	% CDA (DS 2.31)	% MCC (DS 0)	Corresponding DS
1	0	100	0
2	29.87	70.13	0.48
3	53.10	46.90	0.95
4	72.40	27.60	1.43
5	88.07	11.93	1.90
6	100	0	2.31

Table 1. Description of the six standard pellets composing each of the three reference sets employed for the calculation of the calibration functions.

To prepare the standards, CDA and MCC powders were weighed with a Discovery DV215CD Ohau Corporation® analytical balance, and afterwards carefully and thoroughly grinded in an agate mortar in order to obtain homogeneous mixtures. After grinding, the references were pressed under 2 tons for 1 minute to obtain compact pellets, which were kept for 24 hours in a desiccator before performing µATR-FTIR and NIR measurements. Additionally, one CTA pellet was analyzed in a flat area without any sample pretreatment, employing the same methodology used for the pressed pellet references.

2.2 NIR analyses and calibration function

All pressed standard references and the CTA pellet were analyzed by placing them between the spectrometer and a gold-coated glass holder. In all cases, at least 9 measurements per standard were acquired, and the resulting spectra were used as such for the following calculations.

The average 2νOH band maximum wavelength (λ, in nm) per standard pellet was subtracted to the 2νOH band maximum λ in the CTA reference spectrum (registered at 1416 nm) to calculate its average 2νOH band shift.

NIR measurements were collected with a portable NIR spectrometer by Viavi Solutions (JDSU Corporation, Milpitas, CA), a compact device controlled by a portable computer via USB port (Fig. SM.1), registering the diffuse reflectance in the spectral range of 908.1–1676.2 nm (11013.2 –5966.6 cm^{-1}) at a nominal spectral resolution of 6.2 nm. The system is equipped with a linear-variable filter (LVF) as dispersing element, directly connected to a linear 128-pixel indium gallium arsenide (InGaAs) uncooled detector, and employs two tungsten light bulbs as radiation source. The instrument allows for an analysis spot of ca. 3 mm diameter. The sample is directly put in contact with the probe in order to obtain a focal distance of 3 mm.

For the acquisition, first the dark current (D) was measured by placing the spectrometer carefully distant from any surface; then, a raw reflectance reference measurement was acquired from a Spectralon® NIR-reflectance standard S(λ) with known 99% diffuse reflectance values s(λ). Raw reflectance measurements were then recorded from the reference pellets or real films T(λ) by using 100 scan iterations and an integration time of 10.1 ms, resulting in a total of 1.01 second analysis time per measurement. The dark current and reference spectra were kept under 1 minute acquisition times, and the sensor temperature stayed between 36° and 40°C for all measurements. The MicroNIR Pro software (JDSU Corporation, Milpitas, CA) was used for data acquisition.

2.3 μATR-FTIR analyses and calibration function

At least 6 μATR-FTIR spectra were acquired per pressed reference pellet and for the CTA pellet. The spectra were then used without any correction or further manipulation, to calculate the ratio between the absorbance of the νOH band at 3330.6 cm^{-1} (probe band) and the absorbance of the νCOC band at 1020-1039 cm^{-1} (reference band, with the point of the band maximum varying slightly depending on the sample), using the procedure reported by Nunes et al. [1].

μATR-FTIR measurements were acquired from the same areas previously analyzed by NIR, using a Thermo Scientific™ Nicolet™ iN 10MX spectrometer fitted with a mercury–cadmium–telluride (MCT) A-type detector cooled with liquid nitrogen, and a X–Y–Z motorized stage with 1 μm incremental steps. Spectra were recorded in the 4000 to 675 cm^{-1} range using a spectral resolution of 4 cm^{-1}, employing a Ge ATR crystal with an optical aperture of 400 × 400 μm in all cases (except for some real films, where an aperture of 150 × 150 μm was employed), integrating 64 scans for each measurement and for the background, which was acquired before each measurement.

2.4 Real cinematographic films diagnosed with NIR and FTIR functions

A total of 16 developed cinematographic film rolls or film sections with 35 mm gauge and CA polymeric bases (Table 2), kindly provided by the Fondazione Cineteca di Bologna, were analyzed and their DS calculated by using the NIR and μATR-FTIR calibration functions, without any sample preparation.

These 16 samples corresponded to different element typologies (black and white, color, negative and positive elements), manufacturing companies, and covered gradual stages of degradation. Preliminary information about the polymeric base composition was obtained by film inscriptions, as well as

conventional mechanical and visual film examination. The macroscopic condition of the film samples was assessed by registering their degradation effects.

Sample name	***Element typology***		***Condition***
CA1	Positive	Color	Good
CA6	Positive	Black & White	Good
CA7	Negative	Color	Good
Time0	Negative	Color	Good
AA1	Unknown	Color (transparent)	Good
AA4	Negative	Color	Good
AA5	Positive	Color	Good
CT4	Positive	Color	Good
PSATCT-roll3	Positive	Color	Good
CT5	Positive	Color	Good for base, emulsion losses
CT10	Positive	Color	Deformed, faded, slightly rigid
CT11	Positive	Color	Yellowing, slight deformation
CT12	Positive	Color	Yellowing, slight deformation
CT21	Positive	Color	Good for base, emulsion losses
CT24	Positive	Color	Yellowing, slight deformation
CA4	Positive	Color	Brittle

Table 2. Description of the real cinematographic film samples analyzed.

For each analyzed film, at least 3 spectra were acquired with μATR-FTIR and 9-15 NIR measurements were registered on the same region. Regarding the NIR, all real cinematographic film samples were analyzed directly in contact with the CA polymeric bases by placing them between the spectrometer and a gold-coated glass holder. For black and white films, NIR analyses were performed in regions where the emulsion at the opposite side of the film appeared clear, therefore containing low silver particle presence to avoid distortion of the NIR spectra.

The resulting spectra were used without performing any pretreatment or correction to calculate the average 2νOH band shift (NIR) and average νOH/νCOC ratio (μATR-FTIR) per film. These results were then employed for calculating the DS of the CA base in each film with both NIR and μATR-FTIR by solving the corresponding calibration functions. The DS values calculated by the NIR and the μATR-FTIR techniques were compared, and the percentage difference calculated.

3. Results and discussion

3.1 NIR calibration curve for DS calculation

The NIR spectra of the seven standards, corresponding to different DS values, showed characteristic spectral profiles in the NIR region between 900 and 1700 nm, in which overtone and combination bands of CH and OH appear (Fig. 2).

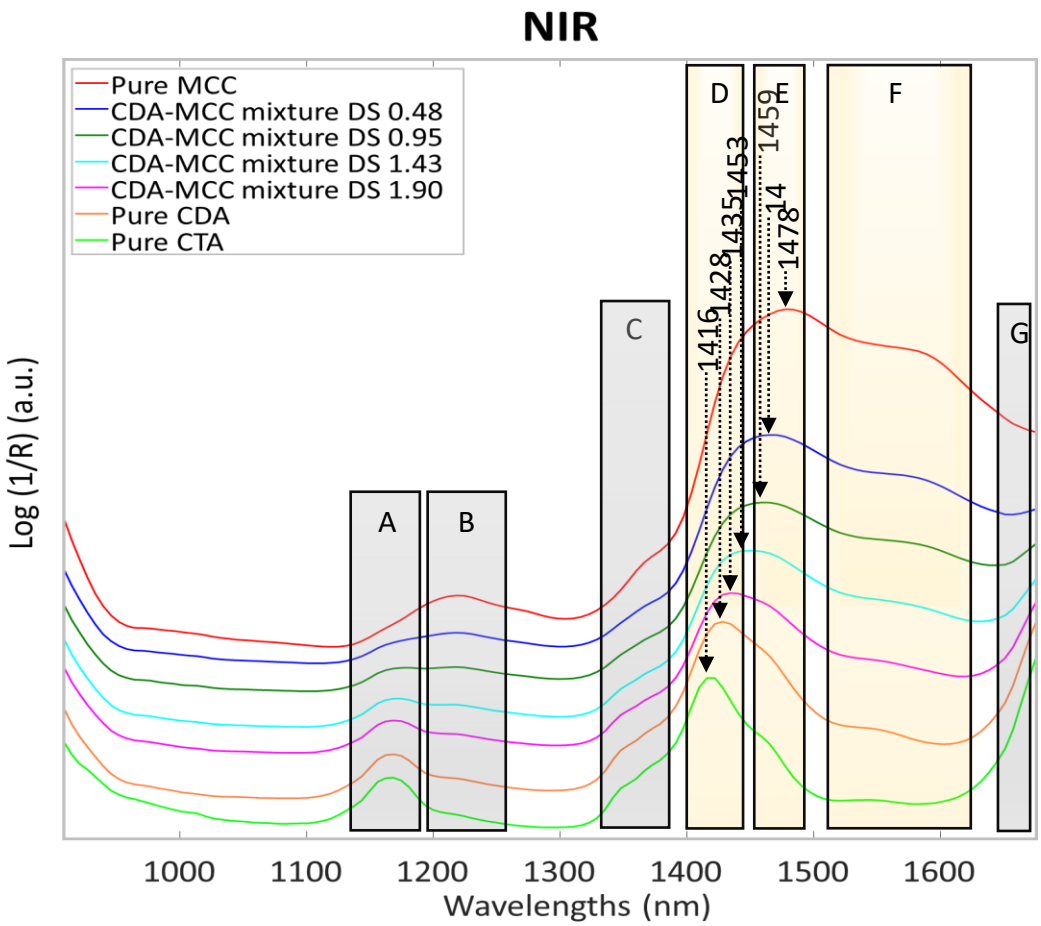

Fig. 2. Selected spectra for each of the seven standard reference materials. The frames indicate the regions (A to G) where different signals appear (assignment is given in Table 3). Regions D to F (highlighted in yellow), corresponding to OH vibrations, were employed for building the calibration functions. A representative approximate maximum for OH bands in each reference has been indicated.

The assignment of the bands in each region of the spectra is shown in Table 3. In particular for the region 1270-1670 nm, deconvolution of the spectra (See Fig. SM.2 to SM.8) allowed to identify the most important components, following the methods reported by Cichosz and Masek [22] and by Mitsui et al.[23] .

Wavelength (Region by letter, peak maxima in nm)	**Assignment**
A.1162-1181	2nd overtone of CH_3 stretching [24]
B. 1218-1273	2nd overtone CH, CH_2 stretching [24-27]

C. 1348 & 1367	1st overtone of CH_3 stretching and bending[24,26,28]
D.1416-1429	1st overtone of OH stretching, amorphous region [21–27, 29-31]
E.1466-1478	1st overtone of OH stretching [27,28,31] in semi-crystalline region [22,24,26,30]
F. 1551-1553, 1577-1603 and 1631-1639	1st overtone of OH stretching [25,26,29] affected by intra and inter chain hydrogen bonds (3OH···O5 and 2OH···O6) in the crystalline region [22-24,28,30,32]
G.1670	1st overtone of CH stretching [21,24-27,32]

Table 3. Interpretation of the NIR spectra for the seven standards shown in Fig. 2, divided by regions (letters A-G).

The changes observed in the spectra with the increasing DS followed specific trends. One of the most notable features is the behavior of the signals at ca. 1162-1181 nm and 1218-1273 nm, attributed to the contribution of methyl group (CH_3) vibrations, and methine and methylene groups (CH, CH_2) respectively [24-27] . It can be noted that, as the DS increases, the relative intensity of the two bands change with a relative increase of the band at 1162-1181 nm ascribable to the higher content of acetate substituents.

Another important trend is related to the changes of the bands appearing between 1400 and 1660 nm. This region is usually attributed to the first overtone of the OH stretching (2ν*OH) which shifts according to the level of crystallinity [22-23]. In our standard samples, as the DS decreases, the maximum of the bands shifts to higher wavelengths (lower frequencies), acquiring also higher relative intensity. A deconvolution of these bands allowed to better understand the changes in the contribution of the different components (Fig. SM.2 to SM.8). A strong signal in the region of 1416-1429 nm corresponds to a higher contribution of hydroxyl groups in the amorphous regions of the polymer; a maximum signal at 1466-1478 nm reflects a higher abundance of hydroxyl groups in semi-crystalline regions, whereas the increase of the signals at 1551-1639 nm is related to more hydroxyl groups involved in intra-molecular hydrogen bonds in crystalline regions of the polymer [22-24,28,30,32] . This accurately reflects the fact that the cellulosic chain decreases in crystallinity with the increase of the DS, as acetyl groups alter the degree of structural organization, modifying inter- and intra-chain interactions [10]. It is known that the occurrence of hydrogen bonds contributes to the shift of the ν*OH fundamental band in the mid-infrared region to lower wavenumbers [33,34] , and this could explain the corresponding shift of the 2ν*OH band in the NIR range to higher wavelengths. Finally, the increase in the relative intensity of the 2ν*OH bands with the decrease of the DS reflects the higher abundance of hydroxyl groups in the cellulosic chain.

A linear trend was observed plotting the DS (y) as a function of the wavelength shift (in nm) of the maximum of the 2ν*OH band in the analyzed standards respect to the wavelength registered for the same band for the CTA reference (x) (Fig. 3).

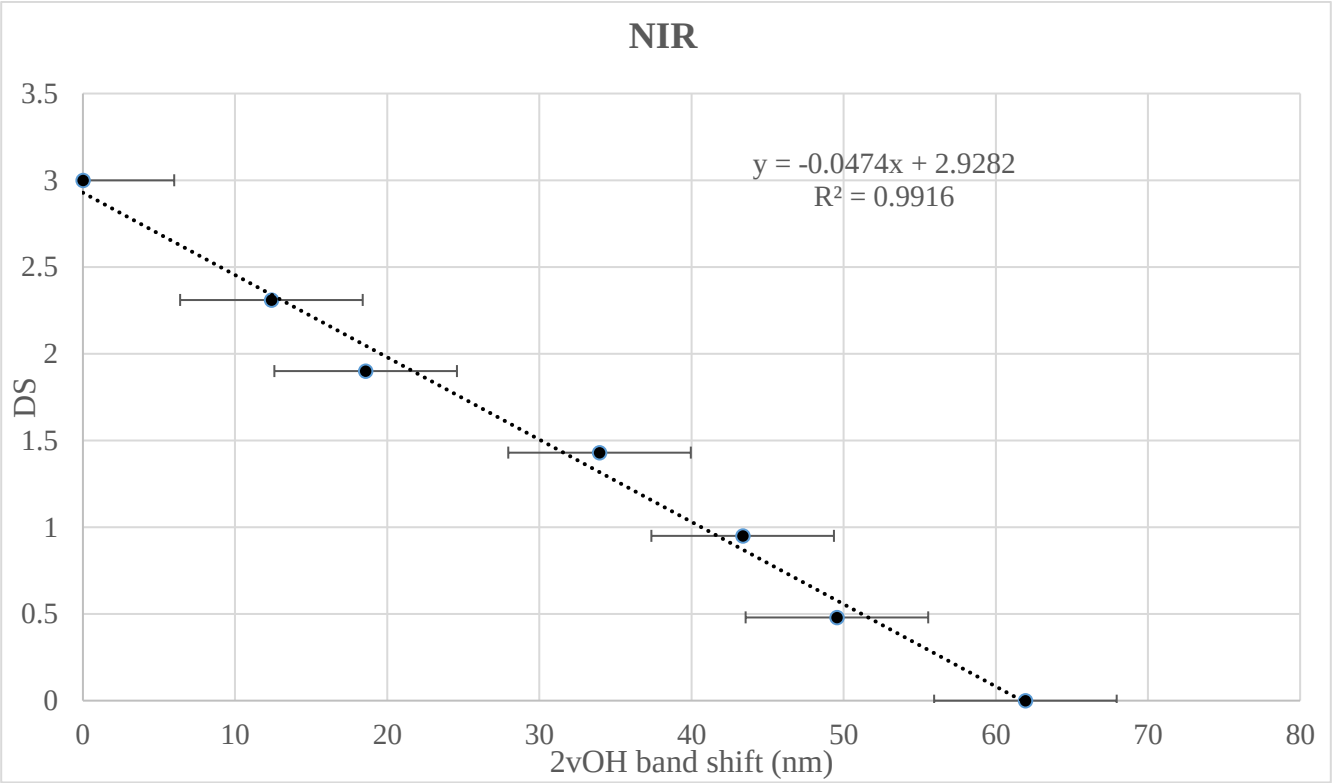

Fig. 3. NIR calibration function showing the DS values as a function of the 2vOH band shift (nm). The band shift is calculated from the reference 2vOH band of CTA.

The correlation between the 2vOH band shift and DS appear robust as confirmed by the high value of the R^2 coefficient. It is worth to note that, even if the standard deviation may be significative for low chemical shift, it is possible to distinguish sample having high and low DS, which is the crucial factor in determining the degradation degree of a CA substrate. Thus, the proposed calibration function permits the application of the portable, fast and cheap system to monitor the change of the DS with the passing of the time on CA based artefacts directly on situ, with no invasiveness toward the objects.

3.2 µATR-FTIR characterization of the standard materials

In order to validate the NIR calibration method on real samples, we created a calibration curve on the same standard samples based on the already established method proposed by [1], based on µATR-FTIR measurements.
The results are in accordance with what have been already published and are summarized in the Supplementary Material (See Fig.SM.9 and related text). The band assignment of the fundamental mid-infrared bands for CTA, CDA and MCC are reported in Table SM.1.

The obtained results that a robust quadratic correlation (R^2=0.98) may be achieved between the DS (y) and the ratio (x) between the absorbance of the OH stretching at 3330.6 cm^{-1} (probe band) and of the COC stretching at ca. 1030 cm^{-1} (reference band) as previously observed [5] (Fig. 4).

It is worth to note that the method may present some limitations when high DS samples have to be measured. The decrease of the OH signal in high DS samples is also affected by the reduced sensitivity of ATR towards high wavenumbers absorption bands for which the depth of penetration is lower with respect to the band in the low wavenumber region[35,36] .

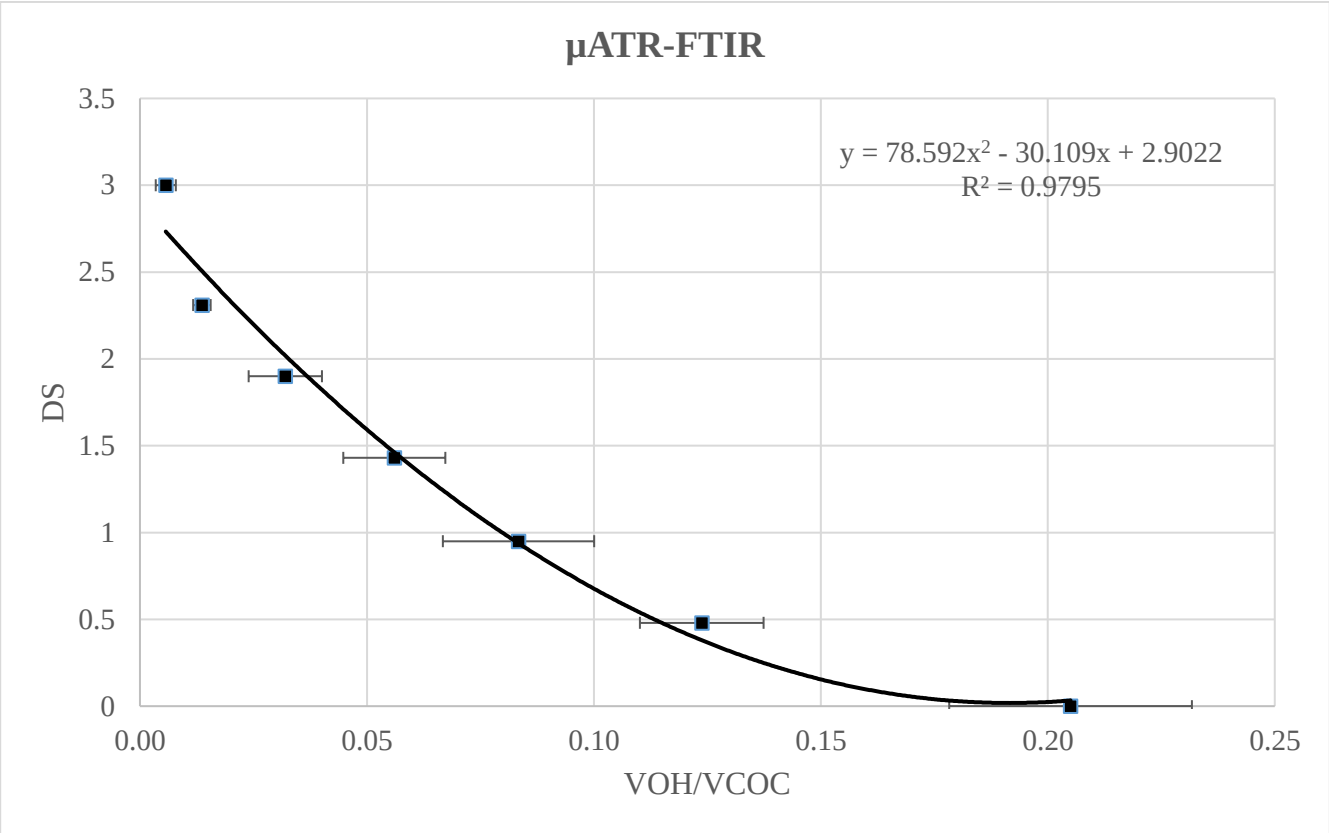

Fig. 4. µATR-FTIR calibration function showing the DS as a function of the band ratio vOH/vCOC.

3.3 Validation of the NIR calibration on real samples

Sixteen cinematographic film samples in differing types of condition were analyzed first with µATR-FTIR, applying the already established calibration method to calculate their DS, and then with the portable NIR in order to validate the new method. Using µATR-FTIR analysis, it was confirmed that in all cases they corresponded to CA bases with TPP as flame retardant.

In order to verify if the NIR spectroscopic features chosen to build the calibration curves may be applied on real samples, the influence of TPP should be taken into consideration. CA film bases may contain from 10 to 20% in weight of triphenyl phosphate (TPP)[37] .
In Fig. 5, the NIR spectrum of pure TPP exhibits its strongest signal at 1131 nm, attributed to the second overtone of aromatic CH stretching [31,38] . As secondary signals, pure TPP showed also weak signals in the range 1300-1500 nm.

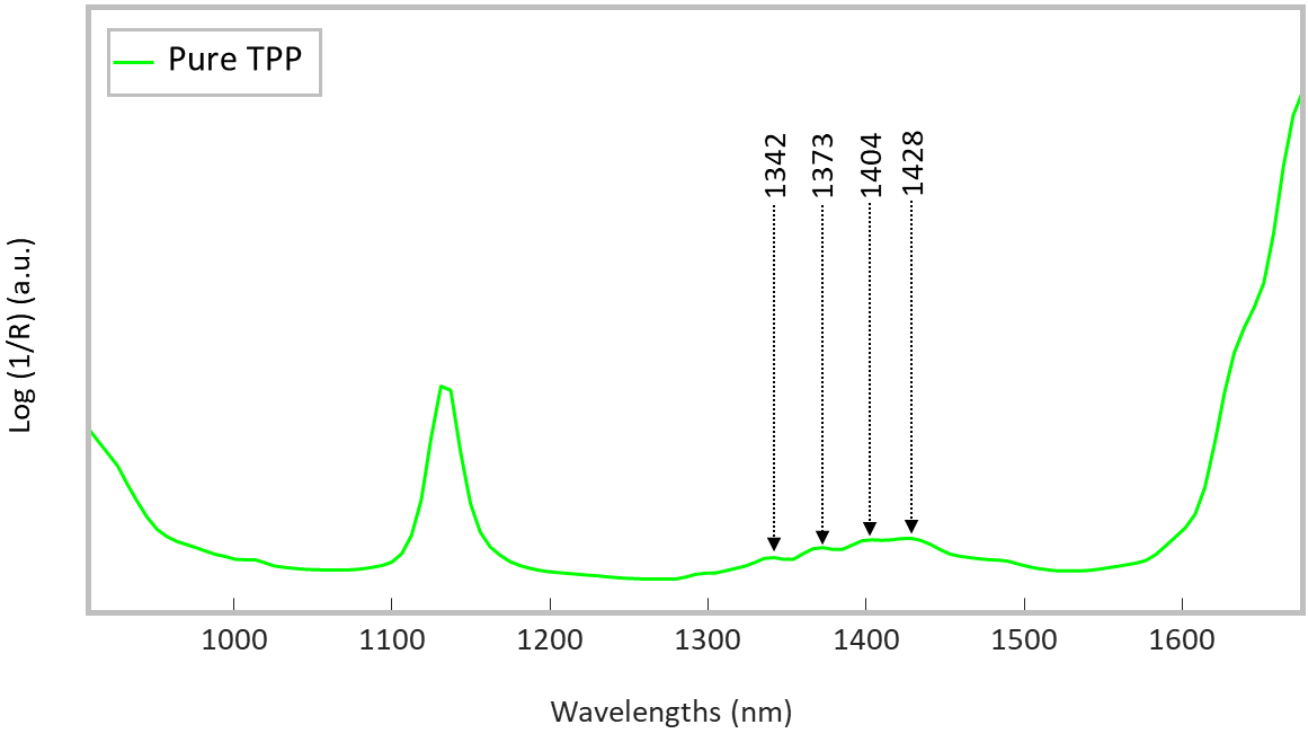

Fig. 5. NIR spectrum of the triphenyl phosphate (TPP) standard.

It is worth to note that due to the low intensity of the TPP bands in the spectral region of interest for the computation of the DS, the presence of the additive in the real samples would not affect the shift of the 2νOH band. In the Supplementary Material, Fig. SM.10 and Table SM.2 report the spectra and band intensities of the 2νOH band in pure MCC, CDA and CTA standards and of the signals of a pure TPP standard occurring in the same region.

An initial overview of the real film macroscopic conditions (Table 2) allowed us to classify nine of them in overall good condition (CA1, CA6, CA7, Time0, AA1, AA4, AA5, CT4 and PSATCT-roll3: showing good flexibility, mechanical resistance, absence of blooming or vinegar odor and no color changes in their emulsion), six in intermediate condition (CT5, CT10, CT11, CT12, CT21 and CT24: with dye fading, base rigidity and distortion) and one sample as heavily degraded (CA4: fragmentary and frail, brittle, with yellowish base).

NIR measurements showed good repeatability, as the 2νOH maximum was registered at the same wavelength in all the measurements performed per sample.

After calculating the DS with both functions, the absolute and percentage difference (being a DS of 3 equal to 100%) between both was assessed (Table 4).

Sample name	Element typology		DS calculated by NIR	DS calculated by µATR-FTIR	DS absolute difference	DS % difference
CA1	Positive	Color	2.63	2.71	0.08	2.7
CA6	Positive	Black & White	2.93	2.73	0.20	6.7
CA7	Negative	Color	2.63	2.78	0.15	5.0
Time0	Negative	Color	2.63	2.82	0.19	6.3
AA1	Unknown	Color (transparent)	2.63	2.77	0.14	4.7
AA4	Negative	Color	2.63	2.86	0.23	7.7
AA5	Positive	Color	2.63	2.79	0.16	5.3
CT4	Positive	Color	2.63	2.77	0.14	4.7
PSATCT-roll3	Positive	Color	2.63	2.75	0.12	4.0
CT5	Positive	Color	2.63	2.82	0.19	6.3
CT10	Positive	Color	1.75	1.70	0.05	1.7
CT11	Positive	Color	1.75	1.60	0.15	5.0
CT12	Positive	Color	1.75	1.50	0.25	8.3
CT21	Positive	Color	2.63	2.51	0.12	4.0
CT24	Positive	Color	1.79	1.90	0.11	3.7
CA4	Positive	Color	0.29	0.09	0.20	6.7

Table 4. Calculation of the DS of the 16 analyzed real cinematographic film samples by using the NIR and µATR-FTIR calibration functions, and comparison between the data obtained by both methods.

Good comparability can be observed among the DS calculated with both methods, with the absolute difference staying below 0.25 and the percentage difference, 8.3%, in all cases. This allowed us to ensure that the DS calculated with the NIR are consistent. The differences may be associated to the different penetration depths in the NIR and MIR regions [11,18-20], and to the low sensitivity of the µATR-FTIR technique in the high wavenumber region due a further reduction of the penetration depths[35,36] .

4.Conclusion

A new diagnostic method for DS measurement of CA film bases using a NIR calibration function was found to be reliable, and its results comparable to those obtained with an already established method based on µATR FTIR measurements.

With the respect to µATR, the deeper penetration of the proposed method allowed to obtain results which may be more representative of the conservation state of the samples, with respect to µATR-FTIR which provided more superficial information. Even if the standard deviation may be significative in particular

for low shifts, the method appears extremely useful to monitor the change of DS, thus of the state of conservation, of CA based objects on site with the advantages of using a cheap and compact system.

This NIR function represents a promising tool for studying thicker supports found in three-dimensional CA objects, including sculptures, combs, jewelry, etc. allowing for the assessment of the condition of the polymer at different spatial locations without the need of destructive or invasive testing.

In conclusion, this method constitutes a simple, fast, inexpensive and non-destructive means to diagnose CA bases in cinematographic films and photographic negatives and seems to have the potential to be employed to other kind of three-dimensional CA artifacts. The system may potentially be used in museums or cinematheques in order to monitor the condition of CA-based objects and define preventive conservation strategies.

Authors' contributions

MVCL: Conceptualization, data curation, analysis, investigation, methodology and writing of the original draft. **EC:** Contributed to the conceptualization, investigation and methodology **GS**: Contributed to conceptualization; reviewed and edited the work. **SP**: Contributed to conceptualization and methodology; reviewed, edited, and provided validation for the work. **EG:** Supported the technical part. **RM**: Supervised the work.

Acknowledgements

We heartily thank the Fondazione Cineteca di Bologna and the specialists from L'Immagine Ritrovata S.r.l. (Marianna de Sanctis, Maura Psichedda and Lara Nobili) for supporting the research and providing the studied samples. We also thank Prof. Maria Joao Melo and Dr Arthur Neves from the Departamento de Química e Departamento de Conservação e Restauro, Faculdade de Ciências e Tecnologia, Universidade NOVA de Lisboa, for providing us the standards and some of the real samples upon which we calculated the calibration curve. Finally, we thank Jan Dariusz Cutajar for proofreading the article.

Funding

This work was supported by the Emilia-Romagna Region [European Social Fund Scholarship for PhD Research Projects; 2014/2020 program. Project title: *RICORDACI-Ricerca sulla conservazione, restauro e diagnosi di film cinematografic*i, approved DGR 886/2016].

Declaration of competing interest

The authors declare that they have no known competing financial interests or personal relationships that could have appeared to influence the work reported in this paper.

Appendix A

Supplementary material related to this article can be found at *(see corresponding file)*

6. Bibliography

[1] S. Nunes, F. Ramacciotti, A. Neves, E.M. Angelin, A.M. Ramos, É. Roldão, N. Wallaszkovits, A.A. Armijo, M.J. Melo, A diagnostic tool for assessing the conservation condition of cellulose nitrate and acetate in heritage collections: quantifying the degree of substitution by infrared spectroscopy, Herit. Sci. 8 (2020) 33. https://doi.org/10.1186/s40494-020-00373-4.

[2] Y. Shashoua, Conservation of plastics: materials science, degradation and preservation, 1. ed, Elsevier, Oxford, 2008.

[3] P. Read, M.-P. Meyer, Restoration of motion picture film, Butterworth-Heinemann, Oxford, 2000.

[4] L. Enticknap, Film Restoration: the Culture and Science of Audiovisual Heritage., Palgrave Macmillan, 2013. http://public.eblib.com/choice/publicfullrecord.aspx?p=1571902 (accessed November 29, 2018).
[5] FilmCare.org, (n.d.). https://www.filmcare.org/ (accessed July 11, 2019).
[6] A. Bereijo, The conservation and preservation of film and magnetic materials (1): film materials, Libr. Rev. 53 (2004) 323–331. https://doi.org/10.1108/00242530410544411.
[7] A.M. Senna, K.M. Novack, V.R. Botaro, Synthesis and characterization of hydrogels from cellulose acetate by esterification crosslinking with EDTA dianhydride, Carbohydr. Polym. 114 (2014) 260–268. https://doi.org/10.1016/j.carbpol.2014.08.017.
[8] J. Mazurek, A. Laganà, V. Dion, S. Etyemez, C. Carta, M.R. Schilling, Investigation of cellulose nitrate and cellulose acetate plastics in museum collections using ion chromatography and size exclusion chromatography, J. Cult. Herit. 35 (2019) 263–270. https://doi.org/10.1016/j.culher.2018.05.011.
[9] H. Kono, H. Hashimoto, Y. Shimizu, NMR characterization of cellulose acetate: Chemical shift assignments, substituent effects, and chemical shift additivity, Carbohydr. Polym. 118 (2015) 91–100. https://doi.org/10.1016/j.carbpol.2014.11.004.
[10] P. Fei, L. Liao, B. Cheng, J. Song, Quantitative analysis of cellulose acetate with a high degree of substitution by FTIR and its application, Anal. Methods. 9 (2017) 6194–6201. https://doi.org/10.1039/C7AY02165H.
[11] P. Luan, G.S. Oehrlein, Characterization of Ultrathin Polymer Films Using p-Polarized ATR-FTIR and Its Comparison with XPS, Langmuir. 35 (2019) 4270–4277. https://doi.org/10.1021/acs.langmuir.9b00316.
[12] H.W. Siesler, Basic Principles of Near-Infrared Spectroscopy, in: Handb. -Infrared Anal., 3rd ed., CRC Press, 2007.
[13] S. Zhu, H. Chen, M. Wang, X. Guo, Y. Lei, G. Jin, Plastic solid waste identification system based on near infrared spectroscopy in combination with support vector machine, Adv. Ind. Eng. Polym. Res. 2 (2019) 77–81. https://doi.org/10.1016/j.aiepr.2019.04.001.
[14] F. Ren, Z. Jiang, M. Han, H. Zhang, B. Yun, H. Zhu, Z. Li, NIR-II Fluorescence imaging for cerebrovascular diseases, VIEW. 2 (2021) 20200128. https://doi.org/10.1002/VIW.20200128.
[15] C. Yin, X. Lu, Q. Fan, W. Huang, Organic semiconducting nanomaterials-assisted phototheranostics in near-infrared-II biological window, VIEW. 2 (2021) 20200070. https://doi.org/10.1002/VIW.20200070.
[16] F.C. Clarke, S.V. Hammond, R.D. Jee, A.C. Moffat, Determination of the Information Depth and Sample Size for the Analysis of Pharmaceutical Materials Using Reflectance Near-Infrared Microscopy, Appl. Spectrosc. 56 (2002) 1475–1483. https://doi.org/10.1366/00037020260377797.
[17] J.M. Chalmers, N.J. Everall, S. Ellison, Specular Reflectance: A Convenient Tool for Polymer Characterisation by FTIR-Microscopy?, (n.d.) 14.
[18] E.A. Carter, B. Swarbrick, T.M. Harrison, L. Ronai, Rapid identification of cellulose nitrate and cellulose acetate film in historic photograph collections, Herit. Sci. 8 (2020) 51. https://doi.org/10.1186/s40494-020-00395-y.
[19] E. Catelli, G. Sciutto, S. Prati, M.V. Chavez Lozano, L. Gatti, F. Lugli, S. Silvestrini, S. Benazzi, E. Genorini, R. Mazzeo, A new miniaturised short-wave infrared (SWIR) spectrometer for on-site cultural heritage investigations, Talanta. 218 (2020) 121112. https://doi.org/10.1016/j.talanta.2020.121112.
[20] W. Xu, L. Wang, R. Zhang, X. Sun, L. Huang, H. Su, X. Wei, C.-C. Chen, J. Lou, H. Dai, K. Qian, Diagnosis and prognosis of myocardial infarction on a plasmonic chip, Nat. Commun. 11 (2020) 1654. https://doi.org/10.1038/s41467-020-15487-3.

[21] S. Cichosz, A. Masek, IR Study on Cellulose with the Varied Moisture Contents: Insight into the Supramolecular Structure, Materials. 13 (2020) 4573. https://doi.org/10.3390/ma13204573.
[22] K. Mitsui, T. Inagaki, S. Tsuchikawa, Monitoring of Hydroxyl Groups in Wood during Heat Treatment Using NIR Spectroscopy, Biomacromolecules. 9 (2008) 286–288. https://doi.org/10.1021/bm7008069.
[23] M. Schwanninger, J.C. Rodrigues, K. Fackler, A Review of Band Assignments in near Infrared Spectra of Wood and Wood Components, J. Infrared Spectrosc. 19 (2011) 287–308. https://doi.org/10.1255/jnirs.955.
[24] A. Wójciak, H. Kasprzyk, E. Sikorska, A. Krawczyk, M. Sikorski, A. Wesełucha-Birczyńska, FT-Raman, FT-infrared and NIR spectroscopic characterization of oxygen-delignified kraft pulp treated with hydrogen peroxide under acidic and alkaline conditions, Vib. Spectrosc. 71 (2014) 62–69. https://doi.org/10.1016/j.vibspec.2014.01.007.
[25] X. Li, C. Sun, B. Zhou, Y. He, Determination of Hemicellulose, Cellulose and Lignin in Moso Bamboo by Near Infrared Spectroscopy, Sci. Rep. 5 (2015) 17210. https://doi.org/10.1038/srep17210.
[26] B. Sun, J. Liu, S. Liu, Q. Yang, Application of FT-NIR-DR and FT-IR-ATR spectroscopy to estimate the chemical composition of bamboo (Neosinocalamus affinis Keng), Holzforschung. 65 (2011). https://doi.org/10.1515/hf.2011.075.
[27] R. Risoluti, S. Materazzi, F. Tau, A. Russo, F.S. Romolo, Towards innovation in paper dating: a MicroNIR analytical platform and chemometrics, The Analyst. 143 (2018) 4394–4399. https://doi.org/10.1039/C8AN00871J.
[28] K. Awa, H. Shinzawa, Y. Ozaki, An Effect of Cellulose Crystallinity on the Moisture Absorbability of a Pharmaceutical Tablet Studied by Near-Infrared Spectroscopy, Appl. Spectrosc. 68 (2014) 625–632. https://doi.org/10.1366/13-07273.
[29] T. Inagaki, H.W. Siesler, K. Mitsui, S. Tsuchikawa, Difference of the Crystal Structure of Cellulose in Wood after Hydrothermal and Aging Degradation: A NIR Spectroscopy and XRD Study, Biomacromolecules. 11 (2010) 2300–2305. https://doi.org/10.1021/bm100403y.
[30] R.M. Correia, F. Tosato, E. Domingos, R.R.T. Rodrigues, L.F.M. Aquino, P.R. Filgueiras, V. Lacerda, W. Romão, Portable near infrared spectroscopy applied to quality control of Brazilian coffee, Talanta. 176 (2018) 59–68. https://doi.org/10.1016/j.talanta.2017.08.009.
[31] L.R. Terra, J.V. Roque, C.C. Pola, I.M. Gonçalves, N. de F.F. Soares, R.F. Teófilo, Study of chemical compound spatial distribution in biodegradable active films using NIR hyperspectral imaging and multivariate curve resolution, J. Chemom. 34 (2020). https://doi.org/10.1002/cem.3193.
[32] A. Benazzouz, E. Dudognon, N.T. Correia, V. Molinier, J.-M. Aubry, M. Descamps, Interactions underpinning the plasticization of a polymer matrix: a dynamic and structural analysis of DMP-plasticized cellulose acetate, Cellulose. 24 (2017) 487–503. https://doi.org/10.1007/s10570-016-1148-y.
[33] Y. Guo, P. Wu, Investigation of the hydrogen-bond structure of cellulose diacetate by two-dimensional infrared correlation spectroscopy, Carbohydr. Polym. 74 (2008) 509–513. https://doi.org/10.1016/j.carbpol.2008.04.005.
[34] D. Estupiñán Méndez, T. Allscher, Advantages of External Reflection and Transflection over ATR in the Rapid Material Characterization of Negatives and Films via FTIR Spectroscopy, Polymers. 14 (2022) 808. https://doi.org/10.3390/polym14040808.
[35] M. Picollo, G. Bartolozzi, C. Cucci, M. Galeotti, V. Marchiafava, B. Pizzo, Comparative Study of Fourier Transform Infrared Spectroscopy in Transmission, Attenuated Total Reflection, and Total

Reflection Modes for the Analysis of Plastics in the Cultural Heritage Field, Appl. Spectrosc. 68 (2014) 389–397. https://doi.org/10.1366/13-07199.

[36] K. Takahashi, M. Sasaki, H. Hayakawa, H. Yajima, Y. Oda, Composition of the white precipitate formed on the surface of damaged triacetyl cellulose-based motion picture films, Sci. Rep. 11 (2021) 1502. https://doi.org/10.1038/s41598-020-80498-5.

[37] C.E. Miller, B.E. Eichinger, Determination of Crystallinity and Morphology of Fibrous and Bulk Poly(ethylene terephthalate) by Near-Infrared Diffuse Reflectance Spectroscopy, Appl. Spectrosc. 44 (1990) 496–504. https://doi.org/10.1366/0003702904086173.